Observation of Orbital Resonance Hall Effect in $(TMTSF)_2ClO_4$

Kaya Kobayashi,[1] H. Satsukawa,[2] J. Yamada,[3] T. Terashima,[2] and S. Uji[2]
[1]*Aoyama Gakuin University, Kanagawa 252-5258, Japan*
[2]*National Institute for Material Science, Ibaraki 305-0003, Japan*
[3]*University of Hyogo, Hyogo 678-1297, Japan*
(Received 27 November 2013; published 20 March 2014)

We report the observation of a Hall effect driven by orbital resonance in the quasi-1-dimensional (q1D) organic conductor $(TMTSF)_2ClO_4$. Although a conventional Hall effect is not expected in this class of materials due to their reduced dimensionality, we observed a prominent Hall response at certain orientations of the magnetic field B corresponding to lattice vectors of the constituent molecular chains, known as the magic angles (MAs). We show that this Hall effect can be understood as the response of conducting planes generated by an effective locking of the orbital motion of the charge carriers to the MA driven by an electron-trajectory resonance. This phenomenon supports a class of theories describing the rich behavior of MA phenomena in q1D materials based on altered dimensionality. Furthermore, we observed that the effective carrier density of the conducting planes is exponentially suppressed in large B, which indicates possible density wave formation.

DOI: 10.1103/PhysRevLett.112.116805 PACS numbers: 75.47.-m, 73.63.-b

Emergent low dimensional electronic states have recently attracted significant attention owing to their appeal as both platforms for new fundamental phenomena and potential technological relevance [1]. The engineering of conducting states at the interface of oxide [2] and organic materials [3] has demonstrated the ability to produce new types of 2-dimensional (2D) conducting systems with novel properties. Parallel to this, systems that host naturally occurring lower-dimensional electron systems supported by a highly anisotropic structures have also shown promise for realizing such states, including p-wave superconductivity [4] and spin liquid [5]. Particularly regarding these naturally anisotropic materials, the vital question remains of to what extent such low-dimensional electronic systems are accessible to measurement and utilization and how those dimensional changes modify electronic structure.

Owing to their highly anisotropic and pristine electronic character, organic conductors offer an attractive ground for addressing this issue. Recent examples include the discovery of a layered, linear dispersion 2D electron system in the quasi-2D organic conductor α-$(BEDT\text{-}TTF)_2I_3$ [6], as well as indications of an Fulde-Ferrell-Larkin-Ovchinnikov ground state supported by reduced dimensionality in the tetramethyl-tetraselenafulvalene family [$(TMTSF)_2X$, where X is a monovalent anion] of quasi-1D (q1D) Bechgaard salts [7]. The electronic anisotropy of the latter compounds (which we use in this Letter) arises from the stacking of TMTSF planar molecules that have transfer integrals t along the chainlike direction a, interchain direction b, and interlayer direction c, typically of the order $t_a : t_b : t_c \sim 1 : 0.1 : 0.003$. The most well-studied aspect of anisotropy in these materials is the marked dependence of the magnetoresistance on field orientation, which exhibits dips known as Lebed resonances at the magic angles (MAs), as defined herein. It has been demonstrated [8–10] that such behavior can be interpreted as resonances of electron trajectories in terms of semiclassical Boltzmann transport theory or electronic states in a quantum description [11,12], both of which involve the enhanced motion of electrons in the interlayer direction without modification of the electron trajectories in the intralayer direction. Contrary to these models, we report herein an orbital resonance in the Hall response for $X = ClO_4$. The signal is consistent with 2D conducting planes originating from an orbital resonance of motion along the field direction at the MA distinct from the molecular ab plane. This measurement not only sheds new light on previously unresolved Lebed resonance behavior [13,14] but also establishes the emergence of an orbital resonance-driven Hall effect and an emergent low-dimensional system ripe for further exploration.

Most commonly, the MA effect is observed as a dip structure in the interlayer resistance R_{zz} as a function of angle θ at the MA condition defined as

$$\tan\theta = \frac{B_y}{B_z} = \left(\frac{p}{q}\right)\left(\frac{b}{c}\right), \tag{1}$$

where b and c are lattice constants in the y and z direction, p and q are integers, and θ is measured from the z axis. A microscopic and macroscopic depiction of the crystal are shown inset in Fig. 1; the conducting channels are along $\hat{x}$, and the MA correspond to the molecular lattice vectors $\hat{y}$ and $\hat{z}$. Electronic states propagating along the conducting chains (along $\hat{x}$) are modulated by B; at some θ the modulation is commensurate among separate electronic

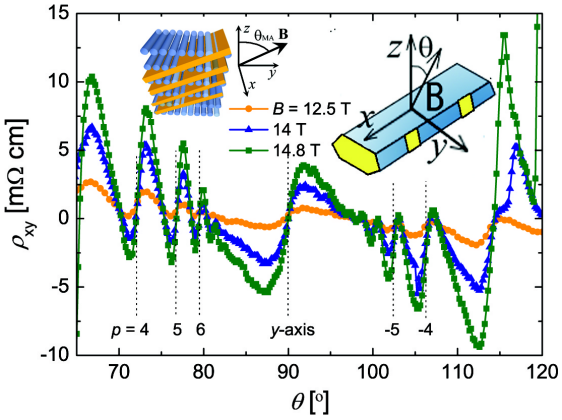

FIG. 1 (color online). The transverse resistivity in the conducting plane ρ_{xy} is plotted as a function of the angle θ of the applied magnetic field B at 12.5 T, 14.0 T, and 14.8 T. The magnetic field is rotated in the yz plane, and θ is measured from the z axis (inset right; visible contact areas shown in gold). The signals show a resonating structure that changes sign at the magic angles, shown as dashed lines with index p. Magic-angle representation is depicted in inset left for $p = 4$.

states and leads to an enhancement (orbital resonance) of the interlayer conductance. Measurements of this effect have served as a useful caliper of the warping of Fermi surfaces of organic q1D conductors [9] and the Fermi velocity [15]. Herein, we focus on the impact of this resonance on the in-plane, off diagonal response ρ_{xy}.

We grew single crystals of $(TMTSF)_2ClO_4$ using the current-controlled electrocrystallization method [16]. We attached 2 gold wires for voltage detection to each side of a needle-like crystal in addition to 2 current terminals that cover both ends (Fig. 1, inset right). Contact is made by carbon paste to avoid reaction at the sample surface. We measured the voltage in the in-plane transverse direction when the electrical current flows along the most conducting direction (the y and x axis in Fig. 1 inset, respectively). We performed the transverse resistivity ρ_{xy} measurement using a lock-in amplifier. We mounted samples on a rotating stage arranged to sit in the center of the 15-T magnet. The rate of cooling for these compounds is important in determining the low T state due to ordering of the tetrahedral anion (ClO_4), which can induce a superlattice potential along the y axis and double the Fermi surface confined in the halved Brillouin zone, triggering drastic changes in the phase diagram [17–19]. Here, we took care to slowly cool the sample, particularly across the anion-ordering temperature $T = 24$ K where we used a rate of 10 mK/min to ensure that the relaxed state was stabilized. We maintained the temperature at $T = 1.6$ K in a pumped-liquid atmosphere of ^{4}He. The high degree of anisotropy in this material often leads to contamination of the in-plane signal by the interlayer resistance [20]. To avoid this contamination, we measured ρ_{xy} over a 2π angular region and subtracted the resistance in π-shifted B. Thus, we could eliminate the interlayer resistivity component, which is an even function of the magnetic field, leaving the B antisymmetric transverse resistivity.

Measurements of ρ_{xy} as a function of θ are shown for 3 different magnetic-field strengths in Fig. 1. Previously, researchers who have conducted experiments in the metallic state at lower B have reported the Hall response to be negligibly small [21]. In this study, we report a large, oscillating $\rho_{xy}(\theta)$. The signal changed sign as θ swept through the y axis, as well as at several orientations above and below the conducting plane. Notably, the additional sign changes in ρ_{xy} occur at the MA defined by Eq. (1). Those θ for several values of p (with $q = 1$) are marked with dashed vertical lines in Fig. 1. Comparison of the different B traces in Fig. 1 shows that increasing B enhances the magnitude of the oscillation but does not alter the θ at which the signal reverses sign and displays extrema. This can be contrasted with the field-induced spin-density wave (FISDW) transition that appears as a sharp increase in the Hall resistivity near 120° at 14.8 T (square symbols) but disperses in B (see also Fig. 3). These features clearly coincide with the MA effects previously observed in R_{xx} and R_{zz}; however, we do not expect an in-plane off-diagonal response in the conventional MA description because those models neglect the in-plane dispersion and describe the effect as purely an interlayer conduction enhancement [8–12].

Near the zeros in $\rho_{xy}(\theta)$ in Fig. 1, we observe a nearly linear angular dependence over several degrees. This angular region is shown expanded for different values of p in Fig. 2(a). When B is aligned with the conducting plane ($B//y$ axis), there is no perpendicular B relative to the conducting plane, so that $\rho_{xy} = 0$. When B slightly deviates from the y axis, the conducting plane experiences a small perpendicular field $B_\perp = B\cos\theta$ in addition to the in-plane magnetic field $B_{//} = B\sin\theta$. Neglecting $B_{//}$, we can plot ρ_{xy} against $B_\perp$ for signals in the vicinity of the y axis. As shown in Fig. 2(c), this yields the linear $\rho_{xy}(B_\perp)$ that one would likely expect for a Hall response. We can also plot $\Delta\rho_{xy} \equiv \rho(\theta) - \rho(\theta_{MA})$ in the vicinity of each MA in the same manner by assuming $B_\perp$ and $B_{//}$ relative to the direction along θ of the MA [see Fig. 2(b)]. As shown in Fig. 2(c), all measurements are linearized in this representation, which indicates a well-defined Hall response from $B_\perp$ in the vicinity of the y axis and the MA.

To further visualize the behavior of $\rho_{xy}(B,\theta)$ in the metallic state, the results over a wide B range at $T = 1.6$ K are displayed in an intensity plot in Fig. 3. The vertical axis represents B from 8.5 to 14.8 T, and the horizontal axis shows θ from 60° to 120°. The color changes from blue to red with increasing ρ_{xy}; this plot gives an expanded view of the angular dependence presented in Fig. 1. For example, the FISDW transitions near 60° and 115°, appearing as dramatic increases of the signal magnitude (dark for 60° and bright for 115°). As noted earlier herein,

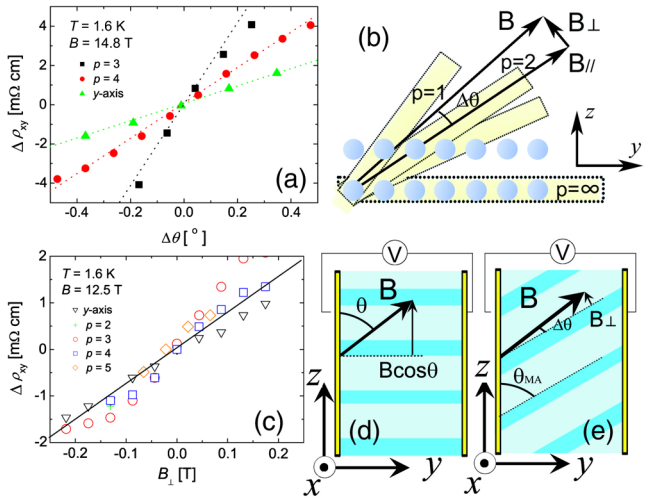

FIG. 2 (color online). (a) Transverse resistivity in the vicinity of Lebed resonance $\Delta\rho_{xy}$ ($p = 3$ and 4) and the y axis as a function of the angular deviation $\Delta\theta$. (b) Definition of $B_\perp$ and $B_{//}$ for a small $\Delta\theta$ about $p = 2$ (other p also shown) for the blue quasi-1-dimensional conducting chains (circles). (c) $\Delta\rho_{xy}$ plotted against $B_\perp$ for $B = 12.5$ T; all data collapse onto a single curve. (d) When the 2-dimensional conducting planes are dominant in the Hall response, the effective magnetic field depends on θ, and the response is proportional to $B\cos\theta$. (e) When MA-formed conducting planes are dominant in conduction, the effective magnetic field in the Hall response is $B_\perp = B\Delta\theta$, consistent with the observations herein.

the FISDW transition disperses to higher θ with increasing B, as marked in Fig. 3 by the white dashed lines. The signal of interest at the MA, however, remains rigidly fixed along the vertical direction (constant θ) with fixed angular width. Another prominent feature of Fig. 3 is the

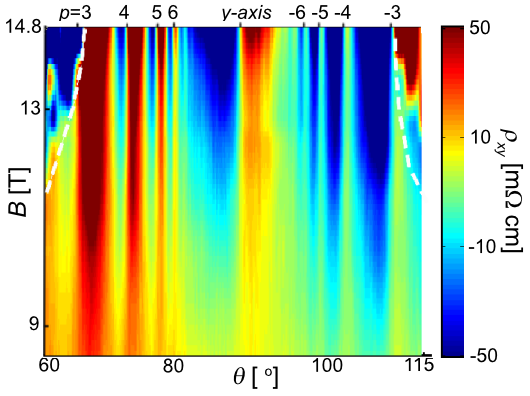

FIG. 3 (color online). Intensity plot of transverse resistivity against the magnetic field strength (vertical) and the magnetic field angle (horizontal; scale bar at right). The structure in the vicinity of the Lebed resonance appears as a nondispersing vertical line in an increasing magnetic field. In contrast, the field-induced spin-density wave (FISDW) transition shows a dispersive angular dependence in an increasing magnetic field (dashed lines).

enhancement of the signals higher than 10 T, which we return to below.

To summarize the results presented earlier herein, $\rho_{xy}(\theta)$ displays a series of resonances at the MA (denoted as angle θ_{MA}), about which the Hall effect has a linear dependence on the deviation $\Delta\theta$ from θ_{MA}. Because a 1D chain cannot support such a response, we consider the possible sources of emergent 2D conduction. One possible candidate is coherent conduction along the ab plane, as depicted in Fig. 2(d). Although this response might be modulated by the interlayer resonance at the MA, as shown in Fig. 2(d), the relevant $B_\perp$ would suggest the coherent plane Hall response $R_H^{\mathrm{coh}} = \cos(\theta)/ne$. The angular dependence of R_H^{coh} would then follow a simple $\cos(\theta)$ dependence and would require a sign change of the Hall response across $\theta = \pi/2$, contrary to the repeated resonances observed herein. Alternatively, it has been discussed in the literature that when B is in the vicinity of the MA condition, electronic motion effectively "locks in" along the MA, as depicted microscopically in Fig. 2(b). Considering the geometry of the transport measurement, as shown in Fig. 2(e), this effect would give rise to an MA Hall response $R_H^{\mathrm{MA}} = \Delta\theta\sin(\theta_{\mathrm{MA}})/ne$, where a linear dependence on $\Delta\theta$ arises due to the small $B_\perp$ at each MA (the dependence on θ_{MA} is a result of the contact geometry measuring along $\hat{y}$). Comparing these possibilities with the experimental results depicted in Figs. 1, 2(a), and 2(c), R_H^{MA} appears to naturally account for the observed linear $\Delta\theta$ dependence we observed at each MA. Further, the approximate equality of the magnitude of R_H^{MA} for different θ_{MA} can be understood as the observed θ_{MA} being confined within approximately $\pm 20°$ of the y axis, where the variation in $\sin(\theta_{\mathrm{MA}})$ is small (within our measurement uncertainty). Thus, we suggest that the Hall response observed in this study originates from the MA lock-in effect, representing a contribution to the Hall effect based on orbital resonance. We propose that orbital resonance triggers the formation of the new conducting planes of $\hat{B}$ and $\hat{x}$. This behavior surpasses that of the enhanced interlayer conduction regime used to explain the typical angular effect in the magnetoconductivity of q1D conductors [22] and favors a dimensionally driven mechanism that has not been considered in the literature thus far, to our knowledge. This result highlights the importance of orbital resonance effects on electronic states in q1D conductors. We note a slight asymmetry of $\rho_{xy}(\theta)$ about $\theta = 90°$, which was not expected from symmetry and could potentially occur due to the anion potential (as in the case of density wave transitions [19]); future experiments with varied cooling rates would clarify whether this is so.

Quantitatively, the B dependence of $\Delta\rho_{xy}$ shows several features that merit further study. Figure 4(a) shows $\Delta\rho_{xy}(B_\perp)$ for the y axis resonance and several MA at different B. For each trace, we can define a Hall coefficient $\rho_{\mathrm{co}} \equiv \Delta\rho_{xy}/B_\perp$ in the vicinity of the MA (± 0.2 T). For

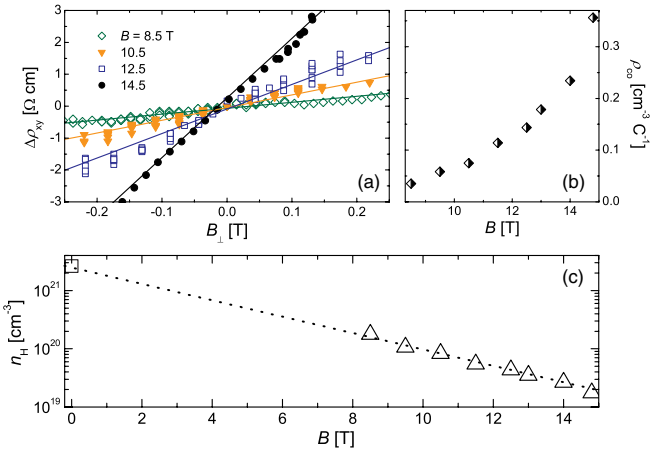

FIG. 4 (color online). (a) Transverse resistivity in the vicinity of the Lebed resonance $\Delta\rho_{xy}$ as a function of $B_\perp$ for different total B at all p indices. (b) The coefficient ρ_{co} as determined by the slope of $\Delta\rho_{xy}(B_\perp)$ at each fixed B is plotted against the magnetic field B. (c) The carrier density n_H derived from ρ_{co} has a strong magnetic field dependence and is fitted by exponential function with $0.3B$ as a fitting parameter (shown as a dashed line).

example, ρ_{co} obtained from the plot of 12.5 T is 0.144 [mΩ cm/T]. This slope, ρ_{co}, for different total magnetic field from 8.5 to 14.8 T, is shown in Fig. 4(b). Making the conventional identification that the carrier number $n_H = B/\rho_{xy}e$, we can extract the effective carrier density of the summed imaginary planes at each B, as shown in Fig 4(c). From 8 to 15 T, we observe an approximately exponential suppression of n_H. Extrapolating this exponential behavior to $B = 0$, we find $n_H(0\ \mathrm{T}) = 2.0 \pm 0.3 \times 10^{21}$ [cm^{-3}], in reasonable agreement with the density expected from the pristine unit cell (2 holes per unit cell is equivalent to 1.3×10^{21} cm^{-3} where a, b, and c are 7.297, 15.422, and 13.522 Å, respectively). This apparent connection of the orbital resonance Hall effect and expected carrier density seems to suggest that most of the carriers participate in conduction along the imaginary planes. Therefore, we suggest that this Hall effect provides a method for probing the carrier density in q1D materials with the additional observation of an unexpected exponential field suppression.

Next, we discuss 2 possible mechanisms for the behavior of $n_H(B)$. First, charge carriers may be localized by their cyclotron motion in strong in-plane fields [23], as has been discussed previously in the context of the MA effects [24] and cuprate superconductors [25]. In the present case, we estimate the z extent of the electron trajectory as $4t_c/(ev_F B_{//})$ for B along the y axis [26]. However, even at the largest B, this trajectory is several nm, which is considerably larger than the interlayer spacing of 13.522 Å. Thus, although $B_{//}$ may play an important role in confinement, it is unlikely to be the source of the carrier localization. An alternate scenario is the possibility of density wave formation in the y direction, as has been discussed based on the temperature dependence observed in interlayer resistance measurements [26]. It has been suggested that B perpendicular to arbitrary current directions favors density wave formation in addition to the FISDW with B along the c axis [27]. This would cause a gap opening in the Fermi surface and would reduce the effective carrier density, consistent with the observations we have presented herein. We hypothesize these observations indicate the presence of a previously unknown density wave transition, which could be tested by future experiments that probe the behavior of this transition at angles further away from the y axis.

The qualitative shape of the resonating structure is similar to the Nernst oscillation at the magic angles reported in the sister compound $X = \mathrm{PF}_6$, although the Hall response was there reported to be unobservable in the metallic state [13,23]. The wide variety of sources of the Nernst response, including vortex motion [28,29], electron-hole compensation [23], and quantum critical points [30], allow for a number of interpretations. The resemblance of our results and the Nernst signal, as reported in sister compound [13,23], indicates that the resonating behavior observed in both signals likely originates from the same mechanism. The analysis of ρ_{xy} that we presented earlier herein leads to straightforward interpretation of "lock-in" behavior for both effects. The observed anomalous behavior of ρ_{xy} appears at higher B compared with the Nernst signal, which may be understood based on the Mott relation [31]. From this relation, $\alpha = (\pi^2 k_B^2 T/3e) \times (\partial \log \sigma(E)/\partial E)_{E=E_F}$, the Seebeck coefficient α is proportional to the logarithmic derivative of the electrical response with respect to energy E (evaluated at the Fermi energy E_F) [31]. This enhanced sensitivity may explain why response in the Nernst effect was more readily observed in lower B when the alteration of the Fermi surface is not as dramatic.

In conclusion, we have observed an oscillating behavior of transverse resistivity $\rho_{xy}(\theta)$ in q1D conductors at the MA condition. The structure of $\rho_{xy}(\theta)$ suggests that the electronic motion can be understood as 2D layers oriented along the MA. Quantitatively, the Hall response reflects the carrier density expected but not previously observed owing to the q1D nature of these materials. This novel Hall response and the emergent 2D conducting superlattice that it probes are ripe for further exploration in terms of the level of 2-dimensionality they exhibit. Measurements of response to external stress and electric potential if the material can be prepared in nanoscale form [32] or thermodynamic measurements [33] may be valuable in evaluating this possibility. The suppression of carriers at high B suggests a transition to an insulating state that warrants further study.

The authors would like to thank P. M. Chaikin and A. G. Lebed for fruitful discussions.

[1] D. L. Cox and D. Pines, MRS Bull. **30**, 425 (2005); N. Curro, Z. Fisk and D. Pines, *ibid.* **30**, 442 (2005).
[2] A. Ohtomo and H. Y. Hwang, Nature (London) **427**, 423 (2004).
[3] J. Takeya *et al.*, Phys. Rev. Lett. **98**, 196804 (2007).
[4] F. L. Pratt, T. Lancaster, S. J. Blundell, and C. Baines, Phys. Rev. Lett. **110**, 107005 (2013).
[5] Y. Shimizu, K. Miyagawa, K. Kanoda, M. Maesato, and G. Saito, Phys. Rev. Lett. **91**, 107001 (2003).
[6] S. Katayama, A. Kobayashi and Y. Suzumura, J. Phys. Soc. Jpn. **75**, 054705 (2006).
[7] I. J. Lee, S. E. Brown, W. G. Clark, M. J. Strouse, M. J. Naughton, W. Kang, and P. M. Chaikin, Phys. Rev. Lett. **88**, 017004 (2001).
[8] A. G. Lebed, JETP Lett. **43**, 174 (1986).
[9] S. J. Blundell and J. Singleton, Phys. Rev. B **53**, 5609 (1996).
[10] T. Osada, S. Kagoshima, and N. Miura, Phys. Rev. B **46**, 1812 (1992).
[11] R. H. McKenzie and P. Moses, Phys. Rev. Lett. **81**, 4492 (1998).
[12] T. Osada and E. Ohmichi, J. Phys. Soc. Jpn. **75**, 051006 (2006).
[13] W. Wu, I. J. Lee and P. M. Chaikin, Phys. Rev. Lett. **91**, 056601 (2003).
[14] E. S. Choi, J. S. Brooks, H. Y. Kang, Y. J. Jo and W. Kang, Phys. Rev. Lett. **95**, 187001 (2005).
[15] K. Kobayashi, M. Saito, E. Ohmichi, and T. Osada, Phys. Rev. Lett. **96**, 126601 (2006).
[16] H. Anzai, J. M. Delrieu, S. Takasaki, S. Nakatsuji, and J. Yamada, J. Cryst. Growth **154**, 145 (1995).
[17] W. Kang, S. T. Hannahs and P. M. Chaikin, Phys. Rev. Lett. **70**, 3091 (1993).
[18] L. P. Gor'kov and A. G. Lebed, Phys. Rev. B **51**, 3285 (1995).
[19] Y. A. Gerasimenko, V. A. Prudkoglyad, A. V. Kornilov, S. V. Sanduleanu, J. S. Qualls, and V. M. Pudalov, JETP Lett. **97**, 419 (2013).
[20] W. Kang, Phys. Rev. B **76**, 193103 (2007).
[21] P. M. Chaikin, M.-Y. Choi, J. F. Kwak, J. S. Brooks, K. P. Martin, M. J, Naughton, E. M. Engler, and R. L. Greene, Phys. Rev. Lett. **51**, 2333 (1983).
[22] W. Kang, T. Osada, Y. J. Jo, and H. Kang, Phys. Rev. Lett. **99**, 017002 (2007).
[23] W. Wu, N. P. Ong, and P. M. Chaikin, Phys. Rev. B **72**, 235116 (2005).
[24] S. P. Strong, D. G. Clarke, and P. W. Anderson, Phys. Rev. Lett. **73**, 1007 (1994).
[25] N. E. Hussey, M. Kibune, H. Nakagawa, N. Miura, Y. Iye, and H. Takagi, Phys. Rev. Lett. **80**, 2909 (1998).
[26] E. I. Chashechkina and P. M. Chaikin, Phys. Rev. Lett. **80**, 2181 (1998).
[27] L. J. Azevedo, J. M. Williams, and S. J. Compton, Phys. Rev. B **28**, 6600 (1983).
[28] Y. Wang, N. P. Ong, Z. A. Xu, T. Kakeshita, S. Uchida, D. A. Bonn, R. Liang, and W. N. Hardy, Phys. Rev. Lett. **88**, 257003 (2002).
[29] Z. A. Xu, N. P. Ong, Y. Wang, T. Kageshita, and S. Uchida, Nature (London) **406**, 486, (2000).
[30] Z. Zhu, H. Yang, B. Fauqué, Y. Kopelevich, and K. Behnia, Nat. Phys. **6**, 26 (2010).
[31] N. F. Mott and H. Jones, *The Theory of the Properties of Metals and Alloys* (Dover, New York, 1958).
[32] K. Kobayashi, H. Koyama, K. Ishikura, and T. Mitsui, Appl. Phys. Lett. **93**, 143114 (2008).
[33] M. J. Naughton, O. H. Chung, M. Chaparala, X. Bu, and P. Coppens, Phys. Rev. Lett. **67**, 3712 (1991).